Indonesian Journal of Electrical Engineering and Computer Science
Vol. 26, No. 2, May 2022, pp. 689~698
ISSN: 2502-4752, DOI: 10.11591/ijeecs.v26.i2.pp689-698

Thermal model developed of high electron mobility transistor AlGaN-GaN

Azzeddine Farti, Abdelkader Touhami
Laboratory of Materials Physics, Microelectronics, Automatic and Thermic, Faculty of Sciences Ain Chock Km 8, University Hassan II, Casablanca, Morocco

Article Info

Article history:

Received Jul 17, 2021
Revised Feb 16, 2022
Accepted May 11, 2022

Keywords:

2-DEG
AlmGa1-mN/GaN HEMTs
Analytical thermal model
Power dissipation
Self-heating

ABSTRACT

The performance of AlGaN-GaN high-electron mobility transistors (HEMTs) is influenced by the self-heating phenomenon, which leads to the power dissipation that is related to the increase of the local temperature of the device. The study of this increasing of the temperature is executed under different parameters, namely, low field mobility, velocity saturation, thermal conductivity of the substrate. A thermal model is developed to study the effect of this phenomenon on the current-voltage characteristics. Among the techniques to minimize the increase in the local temperature, we based on the good choice of the substrate used in the transistor. To highlight this proposal model, we have made a comparable study between the substrates of silicon and sapphire. Our analytical results are in a good agreement with published experimental data.

Corresponding Author:

Azzeddine Farti
Laboratory of Materials Physics, Microelectronics, Automatic and Thermic
Faculty of Sciences Ain Chock Km 8, University Hassan II
Casablanca 5366, Morocco
Email: azzeddine.farti-etu@etu.univh2c.ma

1. INTRODUCTION

The semiconductor devices has contributed in the development of information technologies and communication. An excellent property of electronic devices based on semiconductor materials of the group III-V, among them a high electronic mobility and direct bandgap. In addition, it's able to operate at high frequencies [1]. The high-electron mobility transistors (HEMT) based on AlGaN-GaN have become very strong in recent years for the operating at high temperature, high frequency and high voltage [2]–[6]. This is due to the good properties of gallium nitrides (GaN), among them; we note that it has a wide band gap, a higher mobility of electron, as well as a very high velocity of saturation [7].

However, the operation of high voltage in high performance GaN integrated in circuit for example, low-noise amplifiers voltage controlled oscillators have been indicated [8]. This is due to a phenomenon that we can call it the self-heating. The electrical properties of the transistor HEMT can affect too such as, velocity of saturation, electron mobility, pinch voltage, breakdown voltage and band gap [9], [10], that is not only influence the electrical characteristics negatively, but also degrade the lifetime of the device according to the Arrhenius equation [11]. One of the factors that have a very interesting influence on the electrical characteristics of the transistor HEMT we mention the self-heating. That is motivates us to develop a theoretical thermal model, in order to study this phenomenon and to look for the most adequate substrate for a minimum power dissipation. In this work, we develop a thermal model, and we verify the evolution of the current voltage (I - V) characteristic under the influence of temperature, then we compare it with the experimental results. Finally we use two substrates sapphire and silicon, and we study the variation of the electrical current-voltage (*I- V*) with a fixed the value of gate voltage applied V_{gs}.

2. Model
2.1. Charge control model

The Figure 1 presents the fundamental structure of transistors HEMTs AlGaN-GaN, that is considered in this analytical model. The three main materials that make up the structure of HEMT are: material with a low bandgap, material with a wide bandgap, and substrate. The formation of concentrations of two dimensional electron gas (2-DEG) carriers, at the AlGaN-GaN hetero-junction, it can be given by the following form [12].

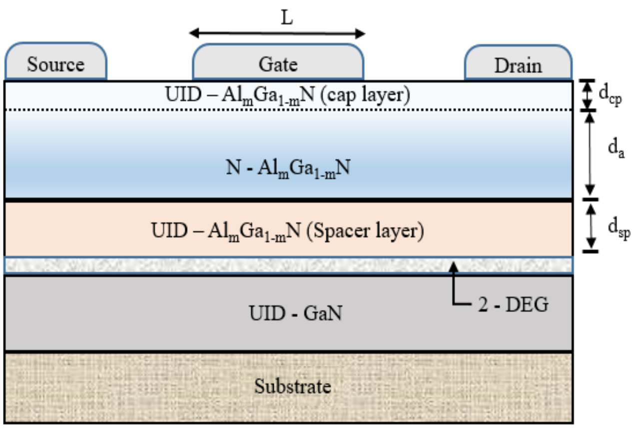

Figure 1. The fundamental structure of HEMT AlGaN-GaN

$$n_s(T,m) = \left(\frac{-K_2(T)+\sqrt{K_2^2(T)+4.K_4(T).\left(V_{gs}-V_{th}(m)-K_1(T)\right)}}{2.K_4(T)}\right)^2 \quad (1)$$

With m present the molar fraction of Aluminum in AlGaN-GaN, and K_1, K_2 and K_3 are three different parameters depend on the temperature *T*.

$$\text{With: } K_4(T) = K_3(T) + \frac{q.d}{\varepsilon(m)} \quad (2)$$

Where, Z $\varepsilon(m)$ and q are the gate width, the dielectric constant of $Al_mGa_{1-m}N$ and the electron charge respectively, $(d = d_a + d_{cp} + d_{sp})$ d_a is the doped layer thickness of the n-AlGaN, d_{sp} and d_{cp} are the thickness of the spacer layer and the cover layer of the undoped layer thickness of d'$Al_mGa_{1-m}N$, respectively, $V_{th}(m)$ is threshold voltage is given by [13].

$$V_{th}(m) = \phi(m) - \Delta E_C(m) - \frac{q.N_d.d_d^2}{2.\varepsilon(m)} \times \left(1 + \frac{2.d_{cp}}{d_a}\right) - \frac{\sigma_{PZ}(m)}{\varepsilon(m)}.d \quad (3)$$

With N_d $\phi(m)$ ΔE_C, are represent the the doping density of the AlGaN layer, the schottky barrier height, and the conduction band discontinuity between AlGaN and GaN respectively, $\sigma_{PZ}(m)$ is the charge density induced by the total polarization can be calculated as (4) [14].

$$\sigma_{PZ}(m) = \left|P_{PP}(m) + P^{sp}_{Al_mGa_{1-m}N}(m) - P^{sp}_{Al_mGa_{1-m}N}(0)\right| \quad (4)$$

Where $P^{sp}_{Al_mGa_{1-m}N}(m)$ denotes the spontaneous polarizations of $Al_mGa_{1-m}N$, and, $P^{sp}_{Al_mGa_{1-m}N}(0)$ denotes the spontaneous polarizations of GaN, and $P_{PP}(m)$ denotes the piezoelectric polarization defined as (5) [14].

$$P_{PP}(m) = \begin{cases} P^{pz}_{Al_mGa_{1-m}N}(m) & \text{Pour} \quad 0 \leq m < 0.38 \\ P^{pz}_{Al_mGa_{1-m}N}(2.33 - 3.5m) & \text{Pour} \quad 0.38 \leq m \leq 0.67 \\ 0 & \text{Pour} \quad 0.67 < m \leq 1 \end{cases} \tag{5}$$

The spontaneous and piezoelectric expressions are presented in Table 1.

Table 1. Parameters of the Al$_m$Ga$_{1-m}$N-GaN heterostructure

Description	Parameter	Expression
Spontaneous polarization of AlGaN	$P^{sp}_{Al_mGa_{1-m}N}(m)$ C/m^2	$-0.09m - 0.034(1-m) + 0.019m(1-m)$
Piezo-electric polarization of AlGaN	$P^{pz}_{Al_mGa_{1-m}N}(m)$ C/m^2	$mP^{pz}_{AlN}[\varepsilon_b(m)] + (1-m)P^{pz}_{GaN}[\varepsilon_b(m)]$
Piezo-electric polarization of AlN	P^{pz}_{AlN} C/m^2	$-1.808\varepsilon_b(m) + 5.624\varepsilon_b^2(m)$
Piezo-electric polarization of GaN	P^{pz}_{GaN} C/m^2	$-0.918\varepsilon_b(m) + 9.541\varepsilon_b^2(m)$
The basal strain	$\varepsilon_b(m)$	$\frac{((a(0) - a(m)))}{a}(m)$
The lattice constant	$a(m)$ Å	$(0.31986 - 0.00891m)$

2.2. Current–voltage characteristics (Ids - Vds)

By giving a fixe value of gate voltage V_{gs} superior of the threshold voltage V_{th}, the movement of electrons at the interface of AlGaN-GaN is accompanied by the application of the drain voltage V_{ds} greater than zero. The generated of the drain current I_{ds} is given by (6) [15].

$$I_{ds}(T,m,x) = Z.q.\mu(x)\left(n_s(T,m)\frac{dV_C(x)}{dx} + \frac{K_B.T}{q}\frac{dn_s(T,m)}{dx}\right) \tag{6}$$

Where, Z, $V_C(x)$ and K_B are the gate width, the channel potential at position x and Boltzmann's constant respectively, $\mu(x)$ is the field dependent of the mobility determined by (7).

$$\mu(x) = \frac{\mu_0}{\left(1+\frac{(\mu_0.E_C - v_{sat})}{E_C.v_{sat}}.\frac{dV_C(x)}{dx}\right)} \tag{7}$$

Where, v_{sat} μ_0 E_C are indicate the saturation drift velocity, the low-field mobility, the saturation electric field respectively. By variation the bias voltage V_{ds}, the HEMT transistor can be function with two different regimes (linear regime and saturation regime).

2.2.1. The linear region $(V_{ds} < V_{dsat})$

View to variation of potential along the 2-DEG channel and with describe it at each position x of the channel, the voltage V_{gs} replace by $V_{gs} - V_C(x)$ in the expression (1) of sheet carrier concentration of two-dimensional electron gas formed at the AlGaN/GaN heterojunction.

$$n_s(T,m,x) = \left(\frac{-K_2(T) + \sqrt{K_2^2(T) + 4.K_4(T,m)\left(V_{gs} - V_{th}(T,m) - V_C(x) - K_1(T)\right)}}{2.K_4(T,m)}\right)^2 \tag{8}$$

Using the following approximation [13].

$$4.K_4(T,m).V_C(x) << K_2^2(T) + 4.K_4(T,m)\left(V_{gs} - V_{th}(T,m) - K_1(T)\right) \tag{9}$$

Referring to (8) a simple expression of the concentration $n_s(T,m)$. This later independent of the position x:

$$n_s(T,m) = \left(\frac{-K_2(T) + \sqrt{K_2^2(T) + 4.K_4(T,m)\left(V_{gs} - V_{th}(T,m) - K_1(T)\right)}}{2.K_4(T,m)}\right)^2 \tag{10}$$

Consequently, the drain current from (8) will be expressed by (11).

$$I_{ds}(T,m,x) = Z.q.\mu(x).\left(n_s(T,m).\frac{dV_C(x)}{dx}\right) \quad (11)$$

We substitute (7) and (10) in the drain current (11), a new equation will appear which describes the drain current at each position x of the channel.

$$I_{ds}(T,m,x) = Z.q.\mu_0.\left(\frac{-K_2(T)+\sqrt{K_2^2(T)+4.K_4(m).\left(V_{gs}-V_{th}(m)-K_1(T)\right)}}{2.K_4(T,m)}\right)^2.\frac{\frac{dV_C(x)}{dx}}{\left(1+\frac{(\mu_0.E_C-v_{sat})}{E_C.v_{sat}}.\frac{dV_C(x)}{dx}\right)} \quad (12)$$

The Figure 2 illustrates the equivalent electrical circuit diagram of transistor HEMT AlGaN-GaN, where R_c is the resistance of the 2-DEG channel, R_d and R_s are the parasitic resistances of the drain and source, respectively.

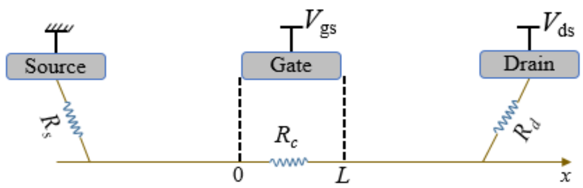

Figure 2. Equivalent electrical schema of the HEMT

From shema in Figure 2 we can conclude the channel potential, for $x = 0$ and $x = L$, and it can be given by (13) and (14).

$$V_C(x)|_{x=0} = I_{ds}.R_s \quad (13)$$

$$V_C(x)|_{x=L} = V_{ds} - (I_{ds} \cdot R_d) \quad (14)$$

The different step of the integration of the (12), along the channel's transistor, and with above boundary conditions can be given by (15) to (20).

$$I_{ds}.\int_0^L \left(1 + \frac{(\mu_0.E_C-v_{sat})}{E_C.v_{sat}}.\frac{dV_C(x)}{dx}\right).dx = Z.q.n_s(T,m).\mu_0.\int_0^L \left(\frac{dV_C(x)}{dx}\right).dx \quad (15)$$

$$I_{ds}\left([x]_0^L + \frac{(\mu_0.E_C-v_{sat})}{E_C.v_{sat}} \cdot [V_C(x)]_0^L\right) = Z.q.n_s(T,m).\mu_0.[V_C(x)]_0^L \quad (16)$$

$$-I_{ds}^2.\left(\frac{(\mu_0.E_C-v_{sat})}{E_C.v_{sat}}.(R_s+R_d)\right) + I_{ds}.\left(L + \frac{(\mu_0.E_C-v_{sat})}{E_C.v_{sat}}.V_{ds} + Z.q.n_s(T,m).\mu_0.(R_s+R_d)\right) - Z.q.n_s(T,m).\mu_0.V_{ds} = 0 \quad (17)$$

We put:

$$\alpha_1 = -\left(\frac{(\mu_0.E_C-v_{sat})}{E_C.v_{sat}}.(R_s+R_d)\right) \quad (18)$$

$$\alpha_2 = L + Z.q.\mu_0.(R_s+R_d).\left(\frac{-K_2(T)+\sqrt{K_2^2(T)+4.K_4(T).\left(V_{gs}-V_{th}(T,m)-K_1(T)\right)}}{2.K_4(T)}\right)^2 + \frac{(\mu_0.E_C-v_{sat})}{E_C.v_{sat}}V_{ds} \quad (19)$$

$$\alpha_3 = -Z.q.\mu_0.\left(\frac{-K_2(T)+\sqrt{K_2^2(T)+4.K_4(T,m).\left(V_{gs}-V_{th}(T,m)-K_1(T)\right)}}{2.K_4(T,m)}\right)^2.V_{ds} \quad (20)$$

The drain current I_{ds} expression in linear regime, will be given by the root of (17), and can be illustrated by following form (21).

$$I_{ds} = \frac{-\alpha_2+\sqrt{\alpha_2^2-4.\alpha_1.\alpha_3}}{2\alpha_1} \tag{21}$$

2.2.2. The saturation region $(V_{ds} \geq V_{dsat})$

The free charge carriers (holes and electrons) acquire a velocity of displacement υ proportional to the applied field, by application an electric field in semiconductor. This velocity can be described by the following relation (22).

$$\upsilon = \mu(x).E(x) = \frac{\mu_0}{\left(1+\frac{(\mu_0.E_C-\upsilon_{sat})}{E_C.\upsilon_{sat}}.\frac{dV_C(x)}{dx}\right)} \cdot \frac{dV_C(x)}{dx} \tag{22}$$

At high electric field values, the velocity of the carriers is saturated at the value υ_{sat}. Which have allowed us to replace the velocity υ by υ_{sat} in expression (12) of the drain current I_{ds}.

$$I_{dsat} = Z.q.\upsilon_{sat}\left(\frac{-K_2(T)+\sqrt{K_2^2(T)+4.K_4(T,m)\left(V_{gs}-V_{th}(T,m)-K_1(T)\right)}}{2.K_4(T,m)}\right)^2 \tag{23}$$

In the same way, we replace the voltage V_{ds} by the saturation voltage V_{dsat} in the equations of a_2 and a_3 . In this case, the drain current expression in the regime of saturation can be written in the below form.

$$I_{dsat} = \frac{-\beta_2+\sqrt{\beta_2^2-4.\alpha_1.\beta_3}}{2.\alpha_1} \tag{24}$$

With,

$$\beta_2 = \delta_2 + \frac{(\mu_0.E_C-\upsilon_{sat})}{E_C.\upsilon_{sat}}V_{dsat} \tag{25}$$

and,

$$\beta_3 = \delta_3 \cdot V_{dsat} \tag{26}$$

where,

$$\delta_2 = L + Z.q.\mu_0.(R_s+R_d)\left(\frac{-K_2(T)+\sqrt{K_2^2(T)+4.K_4(T,m).\left(V_{gs}-V_{th}(T,m)-K_1(T)\right)}}{2.K_4(T,m)}\right)^2 \tag{27}$$

$$\delta_3 = -Z.q.\mu_0.\left(\frac{-K_2(T)+\sqrt{K_2^2(T)+4.K_4(T,m).\left(V_{gs}-V_{th}(T,m)-K_1(T)\right)}}{2.K_4(T,m)}\right)^2 \tag{28}$$

To determine the expression of the saturation voltage V_{dsat} we equalize the (23) and (24) of the drain current I_{ds}.

$$\frac{-\beta_2+\sqrt{\beta_2^2-4.\alpha_1.\beta_3}}{2.\alpha_1} = Z.q.\upsilon_{sat}.\left(\frac{-K_2(T)+\sqrt{K_2^2(T)+4.K_4(T,m).\left(V_{gs}-V_{th}(T,m)-K_1(T)\right)}}{2.K_4(T,m)}\right)^2 \tag{29}$$

We put:

$$\delta_1 = 2 \cdot \alpha_1 \cdot Z \cdot q \cdot v_{sat} \left(\frac{-K_2(T) + \sqrt{K_2^2(T) + 4.K_4(T,m)\left(V_{gs} - V_{th}(T,m) - K_1(T)\right)}}{2.K_4(T,m)} \right)^2 \quad (30)$$

In (29) becomes (31).

$$-\beta_2 + \sqrt{\beta_2^2 - 4.\alpha_1.\beta_3} = \delta_1 \quad (31)$$

According to the expressions of β_2 and β_3, (31) becomes (32).

$$\delta_1 = -\left(\delta_2 + \frac{(\mu_0 E_C - v_{sat})}{E_C v_{sat}} V_{dsat}\right) + \sqrt{\left(\delta_2 + \frac{(\mu_0 E_C - v_{sat})}{E_C v_{sat}} V_{dsat}\right)^2 - 4.\alpha_1.\delta_3.V_{dsat}} \quad (32)$$

As a result, the expression of the saturation voltage V_{dsat} can be expressed by (33).

$$V_{dsat} = \frac{-\delta_1.(2.\delta_2 + \delta_1)}{\left(2.\delta_1.\frac{(\mu_0.E_C - v_{sat})}{E_C.v_{sat}} + 4.\alpha_1.\delta_3\right)} \quad (33)$$

2.3. Low-field mobility μ_0

The low field mobility μ_0 has a significant role in the different performances of transistors [16]. Based on the simulation of this thermal model, we have observed that the low field mobility varies with temperature T, which is presented in the (34).

$$\mu_0(T) = \mu_0(300) - \left(10^{-4} \times (T - 300)\right) \quad (34)$$

With $\mu_0(300)$ presents the mobility at a temperature equals 300 Kelvin. We deduce that, the low field mobility is influenced directly by the temperature, when the temperature T rises, the mobility declines, which result to a reduction in the performance of the transistor.

2.4. The saturation drift velocity v_{sat}

Due to the high electric field in electronic devices, the saturation drift velocity v_{sat} plays an important role [17]. According to the (35) below, we have proposed during the simulation of this thermal model the variation of the saturation drift velocity $v_{sat}(T)$ as function of temperature, we can confirm that while the temperature T increases, the saturation drift velocity decreases, which limits the correct functioning of the transistor HEMT in the applications at high temperatures.

$$v_{sat}(T) = v_{sat}(300) - \left(10 \times (T - 300)\right) \quad (35)$$

With $v_{sat}(300)$ presents the saturation drift velocity at to the temperature of 300 Kelvin.

2.5. Thermal conductivity

The quantity of heat transferred in a material is known as the thermal conductivity, which can be expressed in ($W.K^{-1}.m^{-1}$). The thermal conductivity has modeled by a power law as function of temperature as (36).

$$K(T) = k_0 \left(\frac{300}{T}\right)^{\alpha} \text{ [18]} \quad (36)$$

Where α is the power law coefficient, and k_0 present the thermal conductivity at 300 Kelvin. In this manuscript we will focus on the thermal conductivity of the two substrates: silicon and sapphire, then we study the variation of the temperature in the device using these two substrates (silicon and sapphire), and we observe the substrate that has a lower increase of the temperature in the transistors HEMTs. For this, we use the two following as (37) and (38).

$$K_{saphire}(T) = 0.49 \left(\frac{300}{T}\right) \text{ [19]} \quad (37)$$

$$K_{Si}(T) = 1.57\left(\frac{300}{T}\right)^{1.4} \text{ [20]} \quad (38)$$

2.6. Self-heating effect

The power dissipation appears due to the circulation of the drain current in the region of the 2-DEG channel of transistor HEMT. This power produces a heating in the 2-DEG channel that is called the self-heating that is considered the direct reason for the degradation of the mobility of the carriers and the saturation velocity [21]. Consequently, the self-heating is called the channel temperature, its expression can be given by the following form [21].

$$T_{channel}(T,m) = \left(\frac{1-\left(\frac{1-P_{diss}(T,m)}{4\cdot P_0}\right)^4}{\left(\frac{1-P_{diss}(T,m)}{4\cdot P_0}\right)^4}\cdot T_{sub}\right) + T_{sub} \quad (39)$$

Where, P_{diss} and T_{sub} present successively the power dissipation and the substrate temperature in the transistor HEMT, they can be expressed as [21].

$$P_{diss}(T,m) = I_{ds}(T,m)\cdot V_{ds} \quad (40)$$

$$T_{sub}(T,m) = 300 + \lambda\cdot P_{diss}(T,m) \quad (41)$$

With, λ is a parameter depending on the device thermal resistance [13], and P_0 is called the quantity with the power dimension (watts) that can be given by (42).

$$P_0 = \left(\frac{\pi\cdot K(T_{sub})\cdot Z\cdot T_{sub}}{ln\left(\frac{8\cdot t_{sub}}{\pi\cdot L}\right)}\right) \quad (42)$$

Where, $K(T_{sub})$, t_{sub} are the thermal conductivity, and the thickness of the substrate respectively, The important steps that we will follow to determine the current voltage characteristics considering the effects of self-heating are: firstly we calculate the current voltage characteristic (I_{ds}, V_{ds}) in both region (linear and saturate) in ambient temperature using (6) and (10). Then we substitute the product of I_{ds} and V_{ds} in (40) to calculate the power dissipated. Finally, we deduce the channel temperature with which we calculate the current-voltage electrical characteristics influenced by the temperature.

3. RESULTS AND DISCUSSION

Figure 3 presents, the inverse thermal conductivity $\frac{1}{K(T_{sub})}$, as a function of the temperature T for different substrates: sapphire and silicon. According to this figure, we can observe that the inverse of thermal conductivity of sapphire increases more than silicon when the temperature T increases. It noticed that thermal conductivity of the silicon has less influence with temperature variation than the sapphire substrat.

The channel temperature variation as a function of the drain voltage V_{ds} for various values of the gate voltage V_{gs} is showing in the Figure 4, from (40), as long as the drain voltage rises, the power dissipation increases which translates by an increase of the channel temperature.

Figure 5 illustrates the current-voltage (I_{ds}, V_{ds}) characteristics of the HEMT transistor for various variables of gate voltage V_{gs} from 1.5 to -2.5V with a step of 2V using the sapphire substrate and taking in consideration the existence of self heating and the absence of this latter. From this figure, we note that the experimental results [22] shown through the violet dots agree well with our theoretical calculation (in presence of self-heating) confirming the validity of our model. From the same figure we observe a discrepancy ΔI between the current-voltage electrical characteristics with and without self-heating. This can be explained by the growth of the 2-DEG channel temperature, this latter confirmed well by (40) when the drain voltage V_{ds} increases, which allows the discrepancy ΔI appearances.

Figure 6 illustrats the self-heating effects developed by the variation of the drain current I_{ds} as a function of the drain voltage V_{ds} while the value of the gate voltage V_{gs}equaled zero $V_{gs} = 0$ for the substrats sapphire and silicon in the HEMT transistor AlGaN-GaN. It is observed that the production of the devices with the silicon substrate has a high current density instead of using sapphire substrate. This indicate the importance of the thermal management to reach the higher performances of the devices. The calculated results shows a good agreement with the experimental results [23], which means the validation of the proposed model.

In the present calculation the different parametrs used to simulate this current developed model are illustrated in the Table 2. Also the values of parameters K_1, K_2 and K_3 at different temperatures T which calculated by the same method [24]. Using the effective mass $m^* = 0.22m_0$ [25], used too in this developed model are obtained in Table 3.

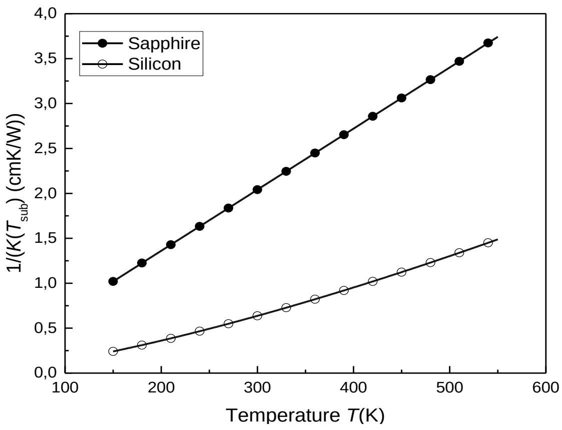

Figure 3. The evolution of the reverse thermal conductivity $\frac{1}{K(T_{sub})}$ (cmK/W)) as a function of the temperature T for different substrates silicon and sapphire

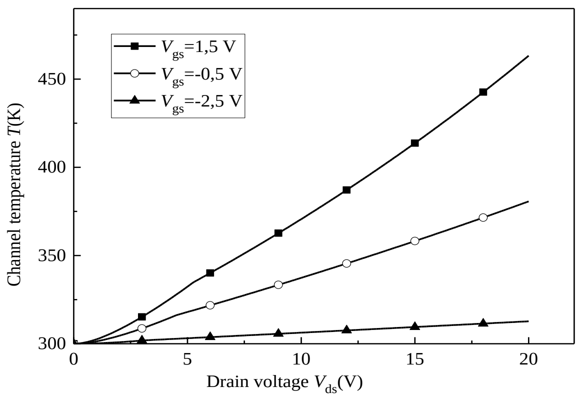

Figure 4. The channel temperature variation versus the drain voltage V_{ds} for various values of the gate voltage V_{gs} for transistor HEMT

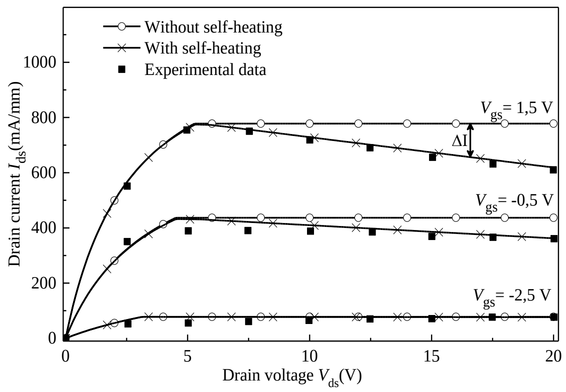

Figure 5. The drain current I_{ds} variation versus the drain voltage V_{ds} for various values of the gate voltage V_{gs}, taking in consideration the absence and the presence of self-heating

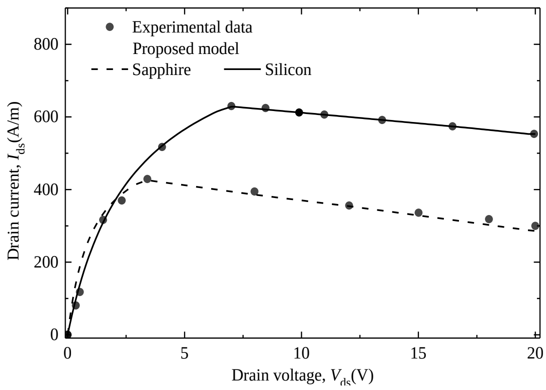

Figure 6. The drain current I_{ds} variation versus the drain voltage V_{ds} for sapphire and silicon substrate materials for L = 0.45 µm and m = 0.2

Table 2. Different parameters used in the present simulation

Parameter	Description	Figure 5	Figure 6
d_{cp}(nm)	Thickness of the undoped cover layer	3	4
d_a(nm)	Thickness of the doped layer	15	16
d_{sp}(nm)	Thickness of the undoped layer	7	6
$Z(\mu m)$	Gate width	15	50
$L(\mu m)$	Gate length	1.5	0.45
$R_s(\Omega)$	Parasitic source resistance	0.6	0.6
$R_d(\Omega)$	Parasitic drain resistance	0.9	0.9

Table 3. Values of the parameters K_1, K_2 and K_3, which calculated by the same method [24] using the effective mass $m^* = 0.22m_0$ [25]

$T(K)$	$K_1(V)$	K_2(Vm)	K_3(Vm^2)
300	-0.2775	1.68742×10^{-8}	-4.2371×10^{-18}
350	-0.328	1.9083×10^{-8}	-5.2147×10^{-18}
400	-0.3792	2.1232×10^{-8}	-6.1660×10^{-18}
450	-0.4313	2.3357×10^{-8}	-7.1058×10^{-18}
470	-0.4512	2.41030×10^{-8}	-7.4352×10^{-18}

4. CONCLUSION

In this work, we investigated the effect of the self-heating on current-voltage electrical characteristics for the transistor HEMT based on GaN. Firstly, we studied the self-heating effect for one substrate, then, we used two substrates to choose the coldest substrate to be used in a high voltage functionning. To highlight the validity and the confirmation of our proposed model, we conducted a comparative study between the simulation results and experimental measurements, this study proved that there is a good match between them, which confirms the validity of our proposed model.

ACKNOWLEDGEMENTS

This work was performed with the support of author's: Farti Azzeddine and Touhami abdelkader in Faculty of Sciences Ain Chock Km8, University Hassan II, Casablanca Morocco.

REFERENCES

[1] J. Ouchrif, A. Baghdad, A. Sshel, A. Badri, and A. Ballouk, "Investigation of the static current gain for InP/InGaAs single heterojunction bipolar transistor," *Indonesian Journal of Electrical Engineering and Computer Science*, vol. 13, no. 3, p. 1345, Mar. 2019, doi: 10.11591/ijeecs.v13.i3.pp1345-1354.
[2] W. Fu, Y. Xu, B. Yan, B. Zhang, and R. Xu, "Numerical simulation of local doped barrier layer AlGaN/GaN HEMTs," *Superlattices and Microstructures*, vol. 60, pp. 443–452, Aug. 2013, doi: 10.1016/j.spmi.2013.05.017.
[3] S. Vitanov, V. Palankovski, S. Maroldt, and R. Quay, "High-temperature modeling of AlGaN/GaN HEMTs," *Solid-State Electronics*, vol. 54, no. 10, pp. 1105–1112, Oct. 2010, doi: 10.1016/j.sse.2010.05.026.
[4] H. F. Huq and B. Polash, "Physics-based numerical simulation and device characterizations of AlGaN/GaN HEMTs with temperature effects," *Microelectronics Journal*, vol. 42, no. 6, pp. 923–928, Jun. 2011, doi: 10.1016/j.mejo.2011.02.003.
[5] S. Nuttinck *et al.*, "Thermal analysis of AlGaN-GaN power HFETs," *IEEE Transactions on Microwave Theory and Techniques*, vol. 51, no. 12, pp. 2445–2452, Dec. 2003, doi: 10.1109/TMTT.2003.819192.
[6] E. Barmala, "Design and simulate a doherty power amplifier using GaAs technology for telecommunication applications," *Indonesian Journal of Electrical Engineering and Computer Science*, vol. 15, no. 2, p. 845, Aug. 2019, doi: 10.11591/ijeecs.v15.i2.pp845-854.
[7] M. A. Huque, S. A. Eliza, T. Rahman, H. F. Huq, and S. K. Islam, "Temperature dependent analytical model for current–voltage characteristics of AlGaN/GaN power HEMT," *Solid-State Electronics*, vol. 53, no. 3, pp. 341–348, Mar. 2009, doi: 10.1016/j.sse.2009.01.004.
[8] J. B. Shealy, J. A. Smart, and J. R. Shealy, "Low-phase noise AlGaN/GaN FET-based voltage controlled oscillators (VCOs)," *IEEE Microwave and Wireless Components Letters*, vol. 11, no. 6, pp. 244–245, Jun. 2001, doi: 10.1109/7260.928926.
[9] S. S. Islam and A. F. M. Anwar, "Self-heating and trapping effects on the RF performance of GaN MESFETs," *IEEE Transactions on Microwave Theory and Techniques*, vol. 52, no. 4, pp. 1229–1236, Apr. 2004, doi: 10.1109/TMTT.2004.825662.
[10] C. H. Oxley and M. J. Uren, "Measurements of unity gain cutoff frequency and saturation velocity of a GaN HEMT transistor," *IEEE Transactions on Electron Devices*, vol. 52, no. 2, pp. 165–169, Feb. 2005, doi: 10.1109/TED.2004.842719.
[11] Y. Zhang, S. Feng, H. Zhu, J. Zhang, and B. Deng, "Two-dimensional transient simulations of the self-heating effects in GaN-based HEMTs," *Microelectronics Reliability*, vol. 53, no. 5, pp. 694–700, May 2013, doi: 10.1016/j.microrel.2013.02.004.
[12] P. Mukhopadhyay, U. Banerjee, A. Bag, S. Ghosh, and D. Biswas, "Influence of growth morphology on electrical and thermal modeling of AlGaN/GaN HEMT on sapphire and silicon," *Solid-State Electronics*, vol. 104, pp. 101–108, Feb. 2015, doi: 10.1016/j.sse.2014.11.017.
[13] M. K. Chattopadhyay and S. Tokekar, "Thermal model for dc characteristics of algan/gan hemts including self-heating effect and non-linear polarization," *Microelectronics Journal*, vol. 39, no. 10, pp. 1181–1188, Oct. 2008, doi: 10.1016/j.mejo.2008.01.043.
[14] V. Fiorentini, F. Bernardini, and O. Ambacher, "Evidence for nonlinear macroscopic polarization in III–V nitride alloy heterostructures," *Applied Physics Letters*, vol. 80, no. 7, pp. 1204–1206, Feb. 2002, doi: 10.1063/1.1448668.
[15] Rashmi, A. Kranti, S. Haldar, and R. S. Gupta, "An accurate charge control model for spontaneous and piezoelectric polarization dependent two-dimensional electron gas sheet charge density of lattice-mismatched AlGaN/GaN HEMTs," *Solid-State Electronics*, vol. 46, no. 5, pp. 621–630, May 2002, doi: 10.1016/S0038-1101(01)00332-X.
[16] A. Mohanbabu, N. Anbuselvan, N. Mohankumar, D. Godwinraj, and C. K. Sarkar, "Modeling of sheet carrier density and microwave frequency characteristics in Spacer based AlGaN/AlN/GaN HEMT devices," *Solid-State Electronics*, vol. 91, pp. 44–52, Jan. 2014, doi: 10.1016/j.sse.2013.09.009.
[17] R. Quay, C. Moglestue, V. Palankovski, and S. Selberherr, "A temperature dependent model for the saturation velocity in semiconductor materials," *Materials Science in Semiconductor Processing*, vol. 3, no. 1–2, pp. 149–155, Mar. 2000, doi: 10.1016/S1369-8001(00)00015-9.
[18] V. Sodan, H. Oprins, S. Stoffels, M. Baelmans, and I. De Wolf, "Influence of field-plate configuration on power dissipation and temperature profiles in AlGaN/GaN on silicon HEMTs," *IEEE Transactions on Electron Devices*, vol. 62, no. 8, pp. 2416–2422, Aug. 2015, doi: 10.1109/TED.2015.2439055.

[19] X. Cheng, M. Li, and Y. Wang, "An analytical model for current–voltage characteristics of AlGaN/GaN HEMTs in presence of self-heating effect," *Solid-State Electronics*, vol. 54, no. 1, pp. 42–47, Jan. 2010, doi: 10.1016/j.sse.2009.09.026.
[20] F. Bonani and G. Ghione, "On the application of the Kirchhoff transformation to the steady-state thermal analysis of semiconductor devices with temperature-dependent and piecewise inhomogeneous thermal conductivity," *Solid-State Electronics*, vol. 38, no. 7, pp. 1409–1412, Jul. 1995, doi: 10.1016/0038-1101(94)00255-E.
[21] P. C. Canfield, S. C. F. Lam, and D. J. Allstot, "Modeling of frequency and temperature effects in GaAs MESFETs," *IEEE Journal of Solid-State Circuits*, vol. 25, no. 1, pp. 299–306, 1990, doi: 10.1109/4.50317.
[22] S. Arulkumaran, T. Egawa, H. Ishikawa, T. Jimbo, and Y. Sano, "Surface passivation effects on AlGaN/GaN high-electron-mobility transistors with SiO2, Si3N4, and silicon oxynitride," *Applied Physics Letters*, vol. 84, no. 4, pp. 613–615, Jan. 2004, doi: 10.1063/1.1642276.
[23] J. Kuzmik, R. Javorka, A. Alam, M. Marso, M. Heuken, and P. Kordos, "Determination of channel temperature in AlGaN/GaN HEMTs grown on sapphire and silicon substrates using DC characterization method," *IEEE Transactions on Electron Devices*, vol. 49, no. 8, pp. 1496–1498, Aug. 2002, doi: 10.1109/TED.2002.801430.
[24] N. DasGupta and A. DasGupta, "An analytical expression for sheet carrier concentration vs gate voltage for HEMT modelling," *Solid-State Electronics*, vol. 36, no. 2, pp. 201–203, Feb. 1993, doi: 10.1016/0038-1101(93)90140-L.
[25] O. Ambacher *et al.*, "Two-dimensional electron gases induced by spontaneous and piezoelectric polarization charges in N- and Ga-face AlGaN/GaN heterostructures," *Journal of Applied Physics*, vol. 85, no. 6, pp. 3222–3233, Mar. 1999, doi: 10.1063/1.369664.

BIOGRAPHIES OF AUTHORS

Azzeddine Farti was born in Sefrou, Morocco, in October 1991. Received his Master degree in Electronics, Signals and Automated Systems from Faculty of Sciences and Technology Fez Morocco, in 2016. He is now Ph.D. student in Microelectronics, under the subject influence of temperature on the electrical characteristics of hemt transistor based on the gan in faculty of science ain chock, University of Hassan II Casablanca Morocco. He can be contacted at email: azzeddine.farti-etu@etu.univh2c.ma.

Abdelkader Touhami obtained his Ph.D. degree in Electronics from the University Hassan II of Casablanca, Morocco. He joined th Faculty of sciences Ain Chock in 1996 where he is currently professor and research scientist in Microelectronics. He is senior principal Microelectronics with Laboratory of Materials Physics, Microelectronics, Automatic and Thermic. He can be contacted at email: abdelkadertouhami2016@gmail.com.